Quantum gas mixtures in different correlation regimes

Miguel Angel Garcia-March[1,2,*] and Thomas Busch[1,3]
[1]*Physics Department, University College Cork, Cork, Ireland*
[2]*Departament d'Estructura i Constituents de la Matèria, Universitat de Barcelona, E-08028 Barcelona, Spain*
[3]*Quantum Systems Unit, Okinawa Institute of Science and Technology Graduate University, Okinawa, Japan*
(Received 10 August 2012; published 25 June 2013)

We present a many-body description for two-component ultracold bosonic gases when one of the species is in the weakly interacting regime and the other is either weakly or strongly interacting. In the one-dimensional limit the latter is a hybrid in which a Tonks-Girardeau gas is immersed in a Bose-Einstein condensate, which is an example of a class of quantum system involving a tunable, superfluid environment. We describe the process of phase separation microscopically as well as semiclassically in both situations and show that quantum correlations are maintained even in the separated phase.

DOI: 10.1103/PhysRevA.87.063633 PACS number(s): 67.85.−d, 03.65.Sq, 03.75.Hh, 03.75.Mn

I. INTRODUCTION

Impurities immersed in ultracold atomic gases have recently been identified as versatile and highly controllable setups for studying quantum correlations in hybrid systems [1]. Demonstrations of single fermions or single ions embedded in a Bose Einstein condensate (BEC) have shown that such systems are experimentally viable [2], and therefore allow one to study a plethora of new quantum phenomena, arising from the interactions between the impurity and the ultracold environment. Better understanding and control of these interactions is already leading to new ideas in quantum information theory [3].

Precursors to these highly controllable hybrid systems have been mesoscopic mixtures of ultracold bosonic gases, which consist of either two different atomic species or two different hyperfine states of the same species [4]. They are commonly available in laboratories worldwide and have allowed one to study mesoscopic quantum dynamics in complex and exotic matter wave states. Such systems have a successful microscopic description based on a two-mode model [5] and can be approximated semiclassically by using a system of coupled Gross-Pitaevskii equations (GPE) [6]. The latter model allows one to describe the stability of the multicomponent system [7] and the process of phase separation [6,8].

In this work we consider a two-component system confined in an effectively one-dimensional (1D) parabolic trap at zero temperature. One of the components is either in the weakly or in the strongly correlated regime, and because of the reduced dimensionality, the latter corresponds to the Tonks-Girardeau (TG) limit [9–11]. The second species is considered to be always in the weakly correlated regime (the BEC regime), and can be seen as a tunable environment for the first component. We show that the quantum correlations within and between the components can be tuned through the coupling between the two species, and describe microscopically the phase separation process that drives the immersed species to the edges of the BEC.

To describe a trapped bosonic quantum gas in one dimension a number of different approaches can be used. The first is to start from a many-body Hamiltonian and expand the field operators into a sufficient number of orbitals. In this representation a direct diagonalization gives a solution in an orbital occupation basis [13], but it can be numerically expensive. A different approach, which successfully reproduces the TG regime as well, is to distribute the atoms over different orbitals and minimize the corresponding multiorbital energy functional associated with all possible configurations to find the ground state of the system (thus permitting the shape of the orbitals to change) [14–17]. In fact, this numerical method allows one to describe also the regime of weak interactions, leading to results coinciding with the GPE approach. Finally, in the case of infinitely strong and repulsive interactions (the TG limit) the atoms can be described by hard sphere bosons and a mapping theorem to a noninteracting Fermi gas exists [9]. This permits one to derive an analytical expression for the wave function in position space and only relies on the knowledge of the solutions of the single-particle problem for the given external potential [9,10,12].

Here we will study the physics of a two-component gas in which one component (*environment*) is always in the weakly interacting limit and the other, smaller component (*system*) can be either weakly or strongly interacting. Both components are trapped in the same one-dimensional harmonic potential (of frequency ω) and their mutual interaction strength can be varied freely. For this we first generalize the direct diagonalization method described in Ref. [13] to mixtures of bosons by expanding the second quantized field operators for both species in a sufficiently large basis of harmonic oscillator functions. This is a viable approach, since even though it is necessary to include a large number of momenta to describe strongly interacting particles correctly, we will consider only a small number and thereby keep the number of modes with finite occupation small. Note that for weak interactions even a large number of bosons at low temperature can be described with a small number of modes. Keeping these points in mind, it is possible to keep the size of the Hilbert space at a numerically manageable level while still describing the physics exactly.

We first use this microscopic description to investigate the phenomenon of phase separation for the two limiting cases when both species are in the weakly interacting regime (the BEC-BEC regime) and when one is in the strongly interacting

*magarciamarch@ecm.ub.edu

regime (the BEC-TG regime). After obtaining the many-body version of the phase separation criterion we show that this process can be interpreted as the excitation of the atoms of the system into higher harmonics and that the symmetry inherent in the external potential means that the system component splits into two parts separated by the atoms of the environment component. The resulting situation is reminiscent of a double-well potential and we demonstrate that the split component maintains its quantum correlations even in the presence of the (potentially large) barrier. Let us point out that the phase separation process for strongly interacting atoms in optical lattices has been studied previously using a generalization of the multiorbital energy functional method [18,19] and the density-functional theory [20].

Since the above approach is computationally restricted by the number of modes that can be considered, we extend the obtained results to the mesoscopic limit by using a semiclassical model similar to the well-known coupled GPE approach [6]. In the BEC-TG regime, however, we show that a GPE coupled to a mean-field equation with a quintic [21,22] rather than a cubic nonlinearity needs to be used, with the nonlinearity of the coupling term depending on the interaction strength between the species. Developing and testing this mean-field model against the exact solutions is of large interest, since it permits one to study dynamical problems, which are currently mostly beyond the reach of other numerical methods [23]. However, this mean-field approach to two-component systems has the same limitations in the strongly correlated regime as in the situation of single component gases, in that it gives a good approximation to the density, while not describing the coherence properties correctly [24].

II. MODEL

For notational simplicity, let us assume that the two atomic components, environment and system, consist of different hyperfine states of the same atomic species and therefore have identical mass m. The intraspecies coupling constants are then given by $g_{E,S} = -2\pi\hbar^2/ma_{1D}^{E,S}$, where the one-dimensional scattering length is defined as $a_{1D}^{E,S} = (-(a_\perp)^2/2a_{E,S})[1 - C(a_{E,S}/a_\perp)]$. Here $a_{E,S}$ is the three-dimensional s-wave scattering length, $a_\perp = \sqrt{2\hbar/m\omega_\perp}$ the radial ground-state size, $\omega_\perp$ the radial trap frequency, and $C = 1.4603$ [25]. The coupling constant between the two components, g_{ES}, is given in a similar fashion in terms of the 1D interspecies scattering length, a_{1D}^{ES}. Describing this mixture in second quantization [5], we first expand the field operators in terms of the eigenfunctions $\phi_n(x)$ of the harmonic potential $V(x) = \frac{1}{2}m\omega^2x^2$ and use $n_{E,S}$ modes for each component,

$$\hat{\psi}_E(x,t) = \sum_{n=1}^{n_E} \hat{a}_n(t)\phi_n(x), \tag{1}$$

$$\hat{\psi}_S(x,t) = \sum_{n=1}^{n_S} \hat{b}_n(t)\phi_n(x). \tag{2}$$

The creation and annihilation operators $\hat{a}_k^\dagger$ and $\hat{a}_k$ satisfy the standard (equal time) bosonic commutation relations $[\hat{a}_k,\hat{a}_l^\dagger] = \delta_{kl}$,$[\hat{a}_k,\hat{a}_l] = [\hat{a}_k^\dagger,\hat{a}_l^\dagger] = 0$ (and similarly for $\hat{b}_k^\dagger$ and $\hat{b}_k$) and the expansion allows us to write the Hamiltonian $\hat{H} = \hat{H}_E + \hat{H}_S + \hat{H}_{\rm int}$ as

$$\hat{H}_E = \sum_{k,l} \hat{a}_k^\dagger \hat{a}_l H_{kl} + \frac{1}{2}\sum_{klmn} \hat{a}_k^\dagger \hat{a}_l^\dagger \hat{a}_m \hat{a}_n V_{klmn}^E, \tag{3a}$$

$$\hat{H}_S = \sum_{k,l} \hat{b}_k^\dagger \hat{b}_l H_{kl} + \frac{1}{2}\sum_{klmn} \hat{b}_k^\dagger \hat{b}_l^\dagger \hat{b}_m \hat{b}_n V_{klmn}^S, \tag{3b}$$

$$\hat{H}_{\rm int} = \frac{1}{2}\sum_{klmn} \hat{a}_k^\dagger \hat{b}_l^\dagger \hat{b}_m \hat{a}_n V_{klmn}^{ES}, \tag{3c}$$

and

$$H_{kl} = \int dx\ \phi_k^*(x) H_{\rm sp} \phi_l(x), \tag{4a}$$

$$V_{klmn}^{E,S} = \frac{g_{E,S}}{2}\int dx\ \phi_k^*(x)\phi_l^*(x)\phi_m(x)\phi_n(x), \tag{4b}$$

$$V_{klmn}^{ES} = g_{ES}\int dx\ \phi_k^*(x)\phi_l^*(x)\phi_m(x)\phi_n(x). \tag{4c}$$

Here $H_{\rm sp}$ is the single-particle Hamiltonian for the harmonic oscillator. Next we expand the ground state $\Psi_0 = \sum_{i=1}^{\Omega} c_i \Phi_i$ as a sum over all Fock vectors given by

$$\Phi_i = D(\hat{a}_1^\dagger)^{N_1^E} \ldots (\hat{a}_{n_E}^\dagger)^{N_{n_E}^E} (\hat{b}_1^\dagger)^{N_1^S} \ldots (\hat{b}_{n_S}^\dagger)^{N_{n_S}^S} \Phi_0, \tag{5}$$

where $D = (N_1^E! \ldots N_{n_E}^E! N_1^I! \ldots N_{n_S}^S!)^{-\frac{1}{2}}$ and Φ_0 is the vacuum. Here $N_1^E, \ldots, N_{n_E}^E$ $(N_1^S, \ldots, N_{n_S}^S)$ are the occupation numbers of the n_E (n_S) modes for the environment (system). The dimension of the Hilbert space is given by $\Omega = \Omega_E\Omega_S$ with $\Omega_{E,S} = (N_{E,S} + n_{E,S} - 1)!/N_{E,S}!(n_{E,S} - 1)!$ where $N^{E,S}$ is the total number of atoms in each species. The fast growth of this space for larger particle or mode numbers is the biggest challenge to the numerical treatment.

III. BEC-BEC REGIME

To anchor our discussion, let us first discuss the limit where the interspecies interaction, g_{ES}, vanishes and the intraspecies interactions, $g_{E,S}$, are small. The two independent components are then each in the weakly correlated regime and it is sufficient to use only a few modes for their description. Indeed, if both components are ideal gases ($g_{E,S} = 0$), the single particle density matrix (SPDM), defined as $\hat{\rho}_E(x,x') = \sum_{k,k'} \phi_k(x)\phi_{k'}(x')\langle\hat{a}_k^\dagger\hat{a}_{k'}\rangle$ and similarly for $\hat{\rho}_S(x,x')$, is simply a Gaussian of width $\alpha = \sqrt{\hbar/m\omega}$. For weak interactions one can therefore assume that most of the atoms still occupy the lowest energy eigenfunction ($N_1^{E,S} \approx N^{E,S}$) and a Gaussian approximation to both eigenstates will be good. Assuming spatial overlap between both components, the ground-state energy can be calculated as

$$E^{\rm hom} = (N_E + N_S)\frac{\hbar\omega}{2} + \frac{g_E}{2\sqrt{2\pi}\alpha}N_E(N_E - 1) + \frac{g_S}{2\sqrt{2\pi}\alpha}N_S(N_S - 1) + \frac{g_{ES}}{\sqrt{2\pi}\alpha}N_E N_S, \tag{6}$$

where we have used that $V_{0000}^{E,S} = g_{E,S}/2\sqrt{2\pi}\alpha$. In general, however, the two species may phase separate, with one of them, say E, remaining in the center of the trap and the other being pushed to the edges. Because the central component will be the one with the lower interaction energy, we will in

the following approximate it using a single Gaussian mode of width α_E in the expansion of the field operator. The other component can then be approximated by a function composed of two displaced Gaussians of width $\frac{\alpha_S}{2}$ [see Fig. 1(d)], which we will call φ_0^{DW}. While in the harmonic oscillator basis the expansion of this state requires a larger number of modes, we use the approximation of φ_0^{DW} as two displaced Gaussians in an effective potential of frequency ω' to find the energy of this state as

$$E^{\text{inh}} = N_E\frac{\hbar\omega}{2} + \frac{g_E}{2\sqrt{2\pi}\alpha_E}N_E(N_E-1) + N_S\frac{\hbar\omega'}{2} + \frac{g_S}{2\sqrt{2\pi}\alpha_S}N_S(N_S-1). \quad (7)$$

To determine the point at which phase separation between the two components happens, we make the reasonable assumption that the atoms occupy the same total (one-dimensional) volume before and after the transition, $\alpha_E + \alpha_S = \alpha$ [8], and minimize the energy with respect to α_E and α_S. This gives $\alpha_E = \alpha/(1+k)$ and $\alpha_S = \alpha/(1+1/k)$, with $k = \sqrt{\frac{g_S}{g_E}\frac{N_S(N_S-1)}{N_E(N_E-1)}}$. Comparing the energies for both cases, and assuming that the change in kinetic energy $\hbar N_S(\omega'-\omega)$ is negligible compared to the overall change in the interaction energies (an assumption we justify below), we obtain the phase separation criterion as

$$g_{ES}N_EN_S > \sqrt{g_E\,g_S}\sqrt{N_E(N_E-1)N_S(N_S-1)}. \quad (8)$$

In the limit of large-particle numbers, $N_{E,S}(N_{E,S}-1) \approx N_{E,S}^2$, this criterion recovers the well-known semiclassical result [6,8]. Note also that it predicts phase separation for any nonzero value of g_{ES} if one of the components consists only of a single particle. If we expand φ_0^{DW} in terms of the eigenfunctions of the harmonic potential $\varphi_0^{DW} = \sum\langle\varphi_0^{DW}|\phi_k\rangle\phi_k$, we can see that the process of phase separation coincides with the occupation of more and more orbitals in the harmonics basis. Consequently, the phase separated species will be the one with the higher coupling constant and the smaller number of atoms, which allows us to assume in the following that $g_S > g_E$. This is also consistent with our earlier approximation of representing the environment component by a single Gaussian mode. Since we already assumed $N_E \gg N_S$, numerical calculations become feasible due to the shape of the environment component not changing substantially after the phase separation ($\alpha_E \approx \alpha$). We can therefore describe it at any time using only a single mode ($\Omega_E = 1$).

Let us consider atoms of mass 87 a.u. in a trap of frequencies $\omega = 2\pi \times 400\,\text{Hz}$ and $\omega_\perp = 100\,\omega$. As an example, we choose the scattering lengths to be $a_E = a_0/10$ and $a_S = 10a_0$, where a_0 is the Bohr radius. The environment consists of $N_E = 300$ particles and we have $N_S = 4$ atoms in the system component, giving $g_E = 10^{-9}\hbar\omega$ and $g_S = 1.01\times10^{-7}\hbar\omega$. To find the ground state we substitute the coefficients obtained from Eq. (4) into the Hamiltonian (3), and diagonalize it in the Fock basis (5). In order to determine a good lower limit for the number of modes that have to be taken into account, we then perform and compare calculations for increasing n_E and n_S until convergence is reached. As expected, we find that, in this limit, taking only a single mode for the environment is sufficient for the mixed and phase-separated situation, but that more modes (in the harmonic oscillator basis) are necessary for the system component in the phase-separated case. In fact, if the interaction between the atoms in the system component is large (the BEC-TG regime) we find convergences to be reached for $n_S = 14$ for the parameters chosen above, which gives a numerically manageable sized Hilbert space. Note that these numbers are similar to the ones used in Deuretzbacher *et al.* [13] for a single-component gas consisting of five atoms.

In Fig. 1 we show the density of the system component and its average occupation of the harmonic oscillator modes for the two cases of overlapping components ($g_{ES} = 0$, upper row) and phase-separated ones ($g_{ES} = \frac{g_S}{2}$, lower row). As expected, for $g_{ES} = 0$ the SPDM for both species is Gaussian [see inset of Fig. 1(a) for the system component] and the energy given by Eq. (6) can be calculated to be $E^{\text{hom}} = 187.0\,\hbar\omega$. The average occupation for the system component $\langle\hat{n}_k\rangle = \langle\hat{b}_k^\dagger\hat{b}_k\rangle$, represented in Fig. 1(a), shows that mainly one momentum component is occupied, which is consistent with the coupling constant being very small. For higher values of g_S higher lying momenta will start showing larger occupation, however, as long as the interactions are small and phase separation has not yet set in, the occupation of the lowest momentum component remains large. Figure 1(b) shows the density of the system component obtained from the SPDM (solid line), which coincides with the semiclassical calculation using a standard mean-field model (GPE, solid line with circled markers).

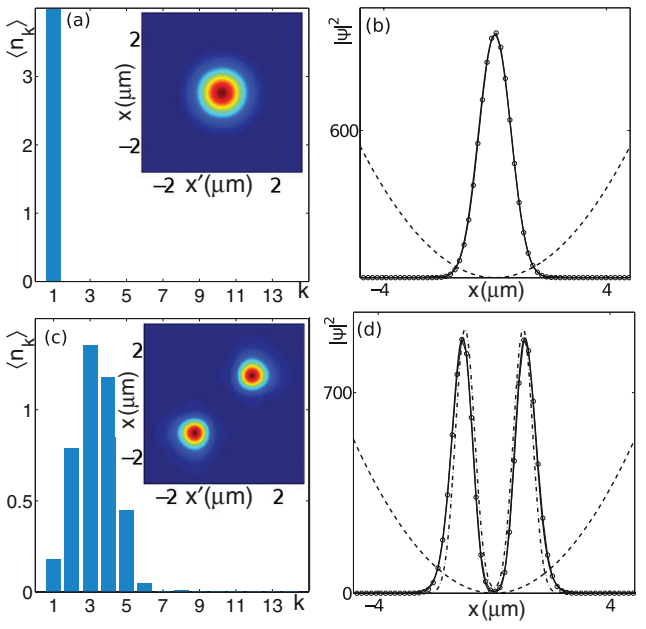

FIG. 1. (Color online) Density and average occupation of orbitals for the system component in the BEC-BEC regime without (upper row) and with (lower row) coupling to the environment. The left column shows the average occupations $\langle\hat{n}_k\rangle$ of the momenta k and the insets show the corresponding SPDMs, spanning a region of $6\,\mu\text{m} \times 6\,\mu\text{m}$. The right column shows the density profiles of the system, with the dashed line being the potential (not drawn to scale), the solid line being the density obtained from the SPDM, and the solid line with circled markers being the one obtained from a semiclassical GPE-GPE simulation. The dash-dotted lines in (d) are the approximate Gaussians located at the minima of the double-well potential $V_{NL}(x) = V(x) + g_{AB}N_B|\phi_0(x)|^2$.

For repulsive interspecies interaction $g_{ES} = \frac{g_S}{2}$ between the components (lower row in Fig. 1) we find the energy for a phase-separated situation to be much smaller than for an overlapping one, $E^{\rm inh} = 191.0\hbar\omega < E^{\rm hom} = 230.8\hbar\omega$, which is in approximate agreement with the numerically found value of $E = 195.0\hbar\omega$. Accordingly, the SPDM in this situation [see Fig. 1(c)] shows a phase-separated gas and occupation of higher momentum modes is found for the system component. The system densities calculated from the SPDM and obtained from the numerical solution of a set of coupled GPEs [7] are displayed in Fig. 1(d) and shows again good agreement. The Gaussian functions used to calculate the energy using Eq. (7) are located at the minima of the effective double-well potential $V_{NL}(x) = V(x) + g_{ES}N_S|\phi_0(x)|^2|$, which are given by $d = \pm\alpha\sqrt{\beta}$, with $\beta = \ln(2g_{ES}N_I/\alpha^3 m\sqrt{\pi}\omega^2)$. Around these points an effective trapping frequency can be approximated as $\omega' = \sqrt{2}\omega\beta$, which leads to the Gaussians having a width of $\alpha' = \sqrt{\hbar/m\omega'}$. The increase in the kinetic energy due to phase separation can then be estimated as $\hbar N_S\omega(1-\sqrt{2}\beta)$, which has to be compared to the change in the interaction energies given by $g_{ES}N_E\,N_S$ and $\sqrt{g_E\,g_S}\sqrt{N_E(N_E-1)N_S(N_S-1)}$. Since the latter is quadratic in the particle number, it is generally much larger except for systems with very small coupling constants and number of atoms.

Let us finally briefly comment on the stability of the phase-separated ground state with respect to a possible symmetry breaking. In the semiclassical limit it is known that symmetry-breaking eigenstates exist, which can have an energy very close to the energy of the symmetric ground state [26–30]. While in the few atom limit and for the symmetric Hamiltonian discussed above, the lowest energy state is the one shown in Figs. 1(c) and 1(d), in actual experiments small perturbations in the potential can break this symmetry. This was shown in [30], where an additional linear potential αx was added to the symmetric trapping potential to show that the asymmetric states experimentally realized in [31] are obtainable from a GPE approach for certain values of the perturbation α.

To demonstrate the stability of the symmetric solution in the few atom limit discussed above, let us consider a tilt ΔV between the minima of the double-well potential $V_{NL}(x) = V(x) + g_{ES}N_S|\phi_0(x)|^2|$. In the symmetric and weakly interacting case the atoms are condensed in a single orbital, which we approximated by the sum of two Gaussians $\varphi_j(x - x_j)$ of width α'. Here x_j $(j = 1,2)$ are the two minima of the potential V_{NL} and the interaction energy is given by $U = (g_S/2)\int|\varphi_j|^4$. To obtain an asymmetric solution the tilt introduced has to be bigger than the gain in interaction energy due to the larger number of atoms overlapping, which is proportional to NU. Therefore a finite gap proportional to the interaction strength exists between the symmetric and asymmetric case for few atom systems, which becomes very small in the GPE mean-field approximation.

IV. BEC-TG REGIME

We now consider the case where the system component is in the TG regime. In Fig. 2 we show the same quantities as before, but now for $N_E = 40$, $a_E = a_0$, and $a_S = 500a_0$, which gives a Lieb-Liniger parameter of $\gamma = 2g_S mL/\hbar^2 N_S = 4.5$ [32], where L is the size of the cloud. This corresponds

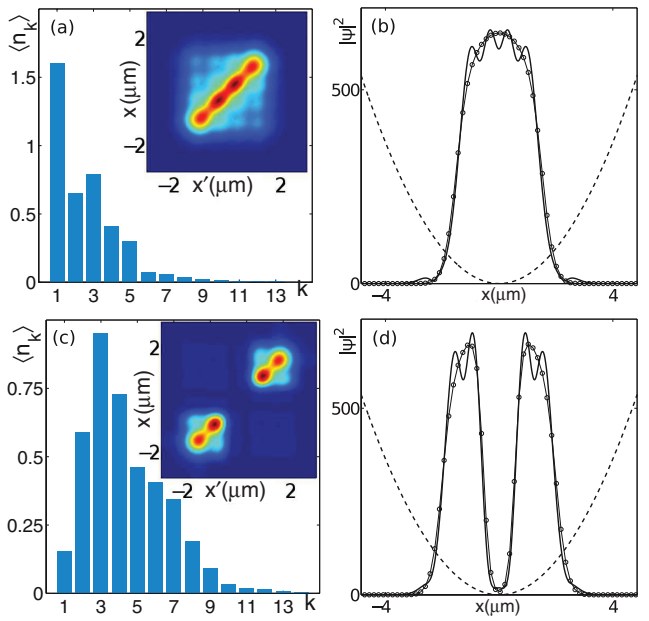

FIG. 2. (Color online) Density and average occupation of orbitals for the system component in the BEC-TG regime without (upper row) and with (lower row) coupling to the environment. Panel layout as in Fig. 1. The semiclassical profiles are obtained using the mean-field equations described in the text.

to the impurities being in the TG regime and we find the interaction coefficients to be $g_E = 10^{-8}\hbar\omega$ and $g_S = 9.6\times 10^{-5}\hbar\omega$. As expected, for no interspecies interaction the SPDM and the momentum distribution for the system resembles that of a TG gas [Fig. 2 (a)]. The density profiles calculated from the microscopic and the semiclassical approach [see below and Fig. 2(b)] show again good agreement. Though the phase separation criterion of Eq. (8) is only approximately valid in this regime, due to the deviations from the Gaussian shapes for the individual components and the fact that the TG gas is not fully condensed into a single orbital, it is still useful away from the precise transition point. The lower row of Fig. 2 shows the situation for $g_{ES} = 0.05g_S$, where phase separation is clearly visible in the SPDM and the momentum distribution shows a shift of the momenta due to the density resembling a higher lying excited state.

To compare the above results with a mean-field model in the semiclassical limit, it is necessary to describe the strongly correlated system component using a quintic nonlinearity in the field equation [21,22]. This approach was developed for single component gases using an appropriate extension of the interaction potential to arbitrary strength [33]. In one dimension this leads to a $|\psi|^6$ term in the energy functional instead of the common $|\psi|^4$ used for BECs in the weakly correlated limit [21,22]. Since for two-species systems the self-interaction properties of the individual components are not changed by the presence of the other one, the mean-field equation for the strongly interacting component requires the $|\psi|^6$ term in the energy functional, whereas the weakly interacting environment retains a quartic term. The nonlinearity of the interspecies interaction term on the other hand, depends on the magnitude of g_{ES}. For small interspecies interactions it is known to be proportional to

the product of the densities of the two components, leading to a standard GPE-like term [6]. Conversely, for stronger interspecies interactions, the interaction potential between both species has to be generalized along the same lines as done for intraspecies scattering [33], leading to a higher order nonlinear coupling term. This allows us to write the coupled mean-field equations as

$$i\hbar\dot{\psi}_S = -\frac{\hbar^2}{2m}\psi_S'' + [V(x) + \tilde{g}_S|\psi_S|^4 + g_{ES}|\psi_E|^p]\psi_S, \quad (9a)$$

$$i\hbar\dot{\psi}_E = -\frac{\hbar^2}{2m}\psi_E'' + [V(x) + g_E|\psi_E|^2 + g_{ES}|\psi_S|^p]\psi_E, \quad (9b)$$

where $\tilde{g}_S = (\pi\hbar)^2/(2m)$ and the exponent of the interspecies coupling term is given by $p = 2$ if $\gamma' = 2g_{ES}mL/\hbar^2 N_S < 1$ and by $p = 4$ in the opposite limit. To show the good agreement between this approach and the microscopic one, we compare the densities obtained by solving the mean-field equations with $p = 2$ in Fig. 2(d) (full line with dotted markers) with the ones obtained from direct diagonalization of the Hamiltonian (3) (full line) for a system with $\gamma' = 0.22$. As expected, calculations for values of g_{ES} larger than the one used in Fig. 2(d) also give good agreement when using $p = 4$, but are not shown here. Note that for mixtures of two strongly interacting species, a similar approach led to a system of two coupled quintic equations [34]. However, let us stress again that these approaches for the TG gas does not describe its coherence properties correctly [24] and a non-mean-field treatment is necessary.

The BEC-TG mixtures behave very differently from the BEC-BEC ones with respect to a possible small asymmetry in the potential. While in the weakly interacting limit the tilt had to be of the order of NU (the increase in energy due to the interactions of all atoms in a single well), in the TG limit the energy increases by about $\hbar\omega'$ with every atom added to the TG localized in one well of V_{NL}. Therefore, the tilt necessary to favor an asymmetric stationary state is much larger in this limit. Summarizing, for different combinations of the inter- and intraspecies interaction energies other solutions can be found as well, some of which can lead to asymmetric distribution in the presence of minimal symmetry breaking [35]. We will discuss the detailed effect of asymmetries in a future work.

Finally, let us return to the microscopic model and discuss the pair correlation function $g^{(2)}(x,x') = \langle\hat{\Psi}^\dagger(x)\hat{\Psi}^\dagger(x')\hat{\Psi}(x')\hat{\Psi}(x)\rangle$, where $\hat{\Psi}(x)$ is the field operator. These correlations give the probability of finding an atom at position x once another atom has been measured at x'. The BEC-BEC case with no interaction between the system and the environment (corresponding to the upper row of Fig. 1) is shown in Fig. 3(a) and the expected Gaussian profile is obtained (again we only show the system component). If the interspecies interaction is strong enough to phase separate the components (lower row in Fig. 1) we find that the two parts of the system density are highly correlated despite being trapped in a deep, effective double-well potential [see Fig. 3(b)]. For the BEC-TG case with no interspecies interaction (corresponding to the upper row in Fig. 2), we recover the well-known hard-sphere behavior for the system component, where two atoms cannot be found at the same point in space [see Fig. 3(c)], which also persists in the phase-separated case [see Fig. 3(d)]. Correlations between the two system peaks are also still visible, however, they show a more complicated structure due to the interspecies interaction.

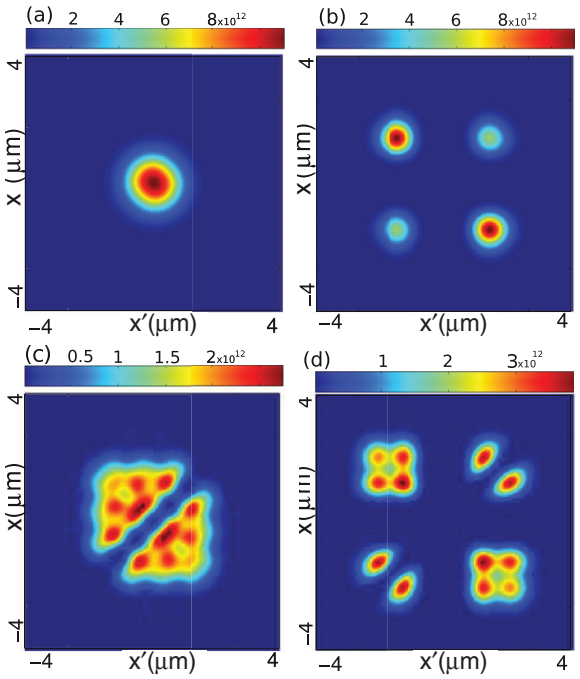

FIG. 3. (Color online) Pair correlation functions $g^{(2)}(x,x')$ for the system component spanning an area of 6 μm × 6 μm. The top row shows the BEC-BEC cases using the same parameters as in Fig. 1 for the situation (a) without and (b) with coupling between species. The lower row shows the BEC-TG regime analogous to the situation in Fig. 2 for the situation (c) without and (d) with coupling between the species.

In conclusion, we have presented a microscopic and a semiclassical model to describe a two-component Bose gas at ultralow temperatures in the one-dimensional limit and allowed for different correlation regimes. This generalizes the known models for interpenetrating ultracold gases to include a significantly larger group of systems, which are currently about to become experimentally available.

Using a microscopic model we have, as a first example, derived a criterion for phase separation, which extends the well-known mean-field result to the mesoscopic limit. We have also presented a semiclassical description of a mixture of ultracold bosons when one of them is highly interacting, and found the nonlinear coupling term between the species to be dependent on the interaction strength. Finally, we have shown that even when the system cloud is split in the phase-separated regime, strong correlations still exist, and the mixture can be seen as a system in which one species is confined in a double-well potential where the barrier formed by the other species. The dynamical properties of such a double-well setting have been studied only with multiconfigurational Hartree-Fock methods by today [36,37] and will be the focus of our ongoing work. Further interesting questions that can be approached with this model include the study of quantum correlations between the system and the environment to study fundamental questions as well as the possibility to use one of the matter waves to engineer the state of the second.

ACKNOWLEDGMENTS

This project was supported by Science Foundation Ireland under Project No. 10/IN.1/I2979. M.A.G.M. acknowledges support from the Grants No. FIS2011-24154 (Ministry of Science and Innovation) and No. 2009SGR-1289 (Generalitat Catalunya). M.A.G.M. acknowledges useful discussions with T. Fogarty.

[1] R. Côté, V. Kharchenko, and M. D. Lukin, Phys. Rev. Lett. **89**, 093001 (2002); M. Bruderer, A. Klein, S. R. Clark, and D. Jaksch, Phys. Rev. A **76**, 011605(R) (2007); J. Goold, H. Doerk, Z. Idziaszek, T. Calarco, and Th. Busch, *ibid.* **81**, 041601(R) (2010); J. Goold, T. Fogarty, N. LoGullo, and M. Paternostro, and Th. Busch, *ibid.* **84**, 063632 (2011).

[2] C. Zipkes *et al.*, Nature (London) **464**, 388 (2010); S. Schmid, A. Harter, and J. H. Denschlag, Phys. Rev. Lett. **105**, 133202 (2010); S. Will, T. Best, S. Braun, U. Schneider, and I. Bloch, *ibid.* **106**, 115305 (2011).

[3] H. Doerk, Z. Idziaszek, and T. Calarco, Phys. Rev. A **81**, 012708 (2010).

[4] C. J. Myatt, E. A. Burt, R. W. Ghrist, E. A. Cornell, and C. E. Wieman, Phys. Rev. Lett. **78**, 586 (1997); D. M. Stamper-Kurn, M. R. Andrews, A. P. Chikkatur, S. Inouye, H. J. Miesner, J. Stenger, and W. Ketterle, *ibid.* **80**, 2027 (1998); S. R. Granade, M. E. Gehm, K. M. OHara, and J. E. Thomas, *ibid.* **88**, 120405 (2002); F. Schreck, L. Khaykovich, K. L. Corwin, G. Ferrari, T. Bourdel, J. Cubizolles, and C. Salomon, *ibid.* **87**, 080403 (2001); A. G. Truscott *et al.*, Science **291**, 2570 (2001).

[5] C. K. Law, H. Pu, N. P. Bigelow, and J. H. Eberly, Phys. Rev. Lett. **79**, 3105 (1997); E. V. Goldstein and P. Meystre, Phys. Rev. A **55**, 2935 (1997); B. D. Esry and Chris H. Greene, *ibid.* **57**, 1265 (1998).

[6] T.-L. Ho and V. B. Shenoy, Phys. Rev. Lett. **77**, 3276 (1996); B. D. Esry, C. H. Greene, J. P. Burke, and J. L. Bohn, *ibid.* **78**, 3594 (1997).

[7] Th. Busch, J. I. Cirac, V. M. Perez-Garcia, and P. Zoller, Phys. Rev. A **56**, 2978 (1997).

[8] P. Ao and S. T. Chui, Phys. Rev. A **58**, 4836 (1998).

[9] M. Girardeau, J. Math. Phys. **1**, 516 (1960).

[10] M. D. Girardeau, E. M. Wright, and J. M. Triscari, Phys. Rev. A **63**, 033601 (2001).

[11] B. Paredes *et al.*, Nature (London) **429**, 277 (2004); T. Kinoshita *et al.*, Science **305**, 1125 (2004).

[12] J. Goold *et al.*, New J. Phys. **12**, 093041 (2010).

[13] F. Deuretzbacher, K. Bongs, K. Sengstock, and D. Pfannkuche, Phys. Rev. A **75**, 013614 (2007).

[14] L. S. Cederbaum and A. I. Strelsov, Phys. Lett. A **318**, 564 (2003).

[15] O. E. Alon and L. S. Cederbaum, Phys. Rev. Lett. **95**, 140402 (2005).

[16] S. Zöllner, H.-D. Meyer, and P. Schmelcher, Phys. Rev. A **74**, 063611 (2006).

[17] S. Zöllner, H.-D. Meyer, and P. Schmelcher, Phys. Rev. A **75**, 043608 (2007).

[18] O. E. Alon, A. I. Streltsov, and L. S. Cederbaum, Phys. Rev. Lett. **97**, 230403 (2006).

[19] S. Zöllner, H.-D. Meyer, and P. Schmelcher, Phys. Rev. A **78**, 013629 (2008).

[20] Y. Hao and S. Chen, Phys. Rev. A **80**, 043608 (2009).

[21] E. B. Kolomeisky and J. P. Straley, Phys. Rev. B **46**, 11749 (1992).

[22] E. B. Kolomeisky, T. J. Newman, J. P. Straley, and X. Qi, Phys. Rev. Lett. **85**, 1146 (2000).

[23] O. E. Alon, A. I. Streltsov, and L. S. Cederbaum, Phys. Rev. A **76**, 062501 (2007).

[24] M. D. Girardeau and E. M. Wright, Phys. Rev. Lett. **84**, 5239 (2000).

[25] M. Olshanii, Phys. Rev. Lett. **81**, 938 (1998).

[26] D. Gordon and C. M. Savage, Phys. Rev. A. **58**, 1440 (1998).

[27] M. Trippenbach, K. Goral, K. Rzazewski, B. Malomed, and Y. B. Band, J. Phys. B: At. Mol. Opt. Phys. **33**, 4017 (2000).

[28] J. G. Kim and E. K. Lee, Phys. Rev. E **65**, 066201 (2002).

[29] A. Balaz and A. I. Nicolin, Phys. Rev. A **85**, 023613 (2012).

[30] R. W. Pattinson, T. P. Billam, S. A. Gardiner, D. J. McCarron, H. W. Cho, S. L. Cornish, N. G. Parker, and N. P. Proukakis, Phys. Rev. A **87**, 013625 (2013).

[31] D. J. McCarron, H. W. Cho, D. L. Jenkin, M. P. Koppinger, and S. L. Cornish, Phys. Rev. A **84**, 011603(R) (2011).

[32] E. Lieb and W. Liniger, Phys. Rev. **130**, 1605 (1963); E. Lieb, *ibid.* **130**, 1616 (1963).

[33] T. D. Lee and C. N. Yang, Phys. Rev. **105**, 1119 (1957); T. D. Lee, K. Huang, and C. N. Yang, *ibid.* **106**, 1135 (1957).

[34] B. Tanatar and K. Erkan, Phys. Rev. A **62**, 053601 (2000).

[35] A. A. Svidzinsky and S. T. Chui, Phys. Rev. A **68**, 013612 (2003).

[36] A. C. Pflanzer, S. Zöllner, and P. Schmelcher, J. Phys. B **42**, 231002 (2009).

[37] A. C. Pflanzer, S. Zöllner, and P. Schmelcher, Phys. Rev. A **81**, 023612 (2010).